THE DISTRIBUTION IN TRANSVERSE MOMENTUM OF 5 GeV/c SECONDARIES PRODUCED AT 53 GeV IN THE CENTRE OF MASS

M.G. ALBROW, D.P. BARBER, A. BOGAERTS, B. BOŠNJAKOVIĆ,
J.R. BROOKS, A.B. CLEGG, F.C. ERNÉ, C.N.P. GEE,
A.D. KANARIS, A. LACOURT, D.H. LOCKE, F.K. LOEBINGER,
P.G. MURPHY, A. RUDGE, J.C. SENS, K. TERWILLIGER*,
and F. Van der VEEN

CERN, Geneva, Switzerland
Foundation for Fundamental Research on Matter (F.O.M.)
Utrecht, The Netherlands
University of Lancaster, U.K.
University of Manchester, U.K.

Received 28 September 1972

Data are reported on the distribution in transverse momentum of 5 GeV/c $\pi^{\pm}$, $K^{\pm}$, p and $\bar{p}$, produced in proton proton collisions at 53 GeV centre of mass energy at the CERN ISR. At this energy the magnitude and p_T dependence of the invariant cross-section appears to be approximately equal to that at 19 GeV accelerator energy (at the same value of the Feynman variable x), for $\pi^{\pm}$ and K^{+} in the range $0.15 < p_T < 0.95$ GeV/c.

We report here results on the distribution in transverse momentum of 5 GeV/c pions, kaons, protons and antiprotons, produced in collisions at the CERN ISR between beams with 26.7 GeV/c momentum each. Tho total energy squared s is 2810 GeV^2, corresponding to a 1500 GeV proton incident on a stationary target. Measurements were performed on secondaries produced in the intervals $0.15 < x < 0.30$ ($x = 2p_L/s^{1/2}$) and $0.15 < P_T < 0.95$ GeV/c, corresponding to production angles in the range $35 < \theta < 180$ mrad.

The apparatus is shown in fig. 1. A partly completed version of the Small Angle Spectrometer (SAS) has been briefly described in ref. [1]. Two septum magnets intercept secondaries produced in a 16 mrad interval of angle, 40% interval in momentum and guide them to a set of three bending magnets placed in the vertical plane above the magnets of ISR ring no. 1. Two gas-filled Cerenkov counters (C_1 and C_2) are placed in front, and one (C_3) behind the bending magnets. Both septum magnets, C_1 and C_2 are mounted on supports which allow for displacement and rotation in the vertical plane. The total accessible angular range is from 25 to 200 mrad. Wire spark chambers with magnetostrictive read-out are placed around the septum magnets and the bending magnets respectively (see fig. 1). They are triggered by a coincidence (ADFIJ) between scintillators placed as shown in fig. 1. Three scintillator telescopes consisting of three counters each are placed around the pipes to measure and monitor the ISR luminosity during the data taking. The location of these luminosity telescopes (one on ring 1, two on ring 2) is indicated in fig. 1. The telescopes also monitor the background in each beam and were used in deciding where to locate each beam for optimum data taking.

For each prevent the spark chamber coordinates, the record of all scintillators, the pulse heights of C_1, C_2 and C_3, the time of flight differences between the first SAS counter and the EG hodoscope (see fig. 1) are recorded on magnetic tape. The data taking is supervised by an extensive package of programs with an on-line IBM 1800 computer.

The data reported here have been taken at 9 settings of angle and momentum of the spectrometer for positive particles and 10 settings for negative particles. Between 10000 and 30000 triggers were recorded at each setting. The trigger rate ranged from about 3/sec at the smallest angles to about 0.2/sec at the largest. At the smallest angles the rates were limited by a dead time of 0.3 sec for recharging the spark chamber high tension circuits.

* On sabbatical leave from the University of Michigan, Ann Arbor, Michigan, USA.

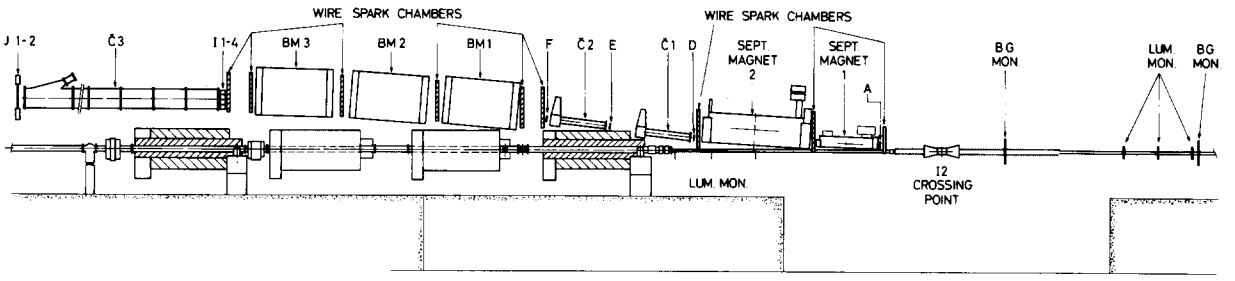

Fig. 1. Side of view of the Small Angle Spectrometer (S.A.S.) on top of beam 1 of the ISR. The moveable part consists of two septum magnets 1 and 2 Cerenkov counters C_1 and C_2 of which both the heights and the tilts can be adjusted. Further downstream are the C magnets BM1, BM2 and BM3 and the 6 meter long Cerenkov counter C_3. The 30 m long spectrometer is triggered by the scintillator counters A, D, F, I and J. The particle trajectories are located by 21 spark chamber planes. Also indicated are the luminosity telescopes under beam 1 and around beam 2, and the beam-gas hodoscope BG.

The main sources of background seen by the spectrometer were secondaries produced in beam/gas and in beam/wall collisions in a region $\approx$ 1 m long centered on the crossing point of the two rings. An indirect consequence of beam/gas collisions is the partial neutralization of the beam by electrons and ions, resulting in a periodic growth of the amplitude of the beam up to the aperture limits of the vacuum chamber. Short bursts of secondaries resulting from these beam/wall effects were suppressed by gating off the SAS trigger when the rate in the luminosity telescope on ring 1 exceeded a prescribed value. The background fraction was determined from the distribution of reconstructed event origins along the beam 1 direction. This distribution showed a pronounced 20 cm wide peak at the crossing point on top of a flat background.The fraction of events substracted as background averaged 3.7% for positive secondaries, 2.3% for negative with an r.m.s. run-to-run scatter of $\approx$ 1% about these values. Within the statistical errors this background was independent of the type of particle detected and of the angle at which SAS was set. This method of background substraction was checked with a hodoscope consisting of four counters around beam 2. This hodoscope, indicated by BG in fig. 1, covered an angular range from $\approx$ 10 to 250 mrad. All SAS events in coincidence with the hodoscope had their origin near the crossing point, indicating that the flat background is due to beam/gas collisions, for which a coincidence between SAS in ring 1 and the monitor hodoscope is ruled out by kinematics. Comparison of the peak heights in the distribution indicated that 96% of the beam-beam events in SAS were in coincidence with the hodoscope.

The events were reconstructed off-line by computing the momentum and angle of production from the spark coordinates and the bonding power (represented by one number, $\int Bdl$, for each magnet) of the fields. Sparks in about two thirds of the chambers were required to define a trajectory. In all data except those taken at 70 – 100 mrad, when the current in the two septum magnets is zero or nearly zero, the momentum was measured twice: once from the triplet chambers around the septum magnets, and once from the doublets around the bending magnets. Further constrains were imposed by requiring the reconstructed tracks to pass through all counters in the trigger. The accuracy in momentum was typically ± 1%; the angle of production was determined with a precision of 2 mrad. The track finding efficiency was typically 50%. In the back half of the spectrometer it was always 90% or better. About half of the remaining 10% was due to scattering of particles against pole pieces of the magnets and the other half due to spark chamber inefficiencies. In the front half only 60% of the tracks could be reconstructed..Investigation of the failures showed that these were mainly due to spark robbing by coincident particles going underneath the septum magnet. A small amount of false triggers was caused by particles going under the first septum magnet in coincidence with a particle in the first trigger counter.

Particles were identified by means of gas Cerenkov counters C_1, C_2 and C_3. The counters C_1 and C_2 (1.55 m long, 12 kg/cm^2 ethylene) counted π's and K's for momenta exceeding 3.8 GeV/c. The proton

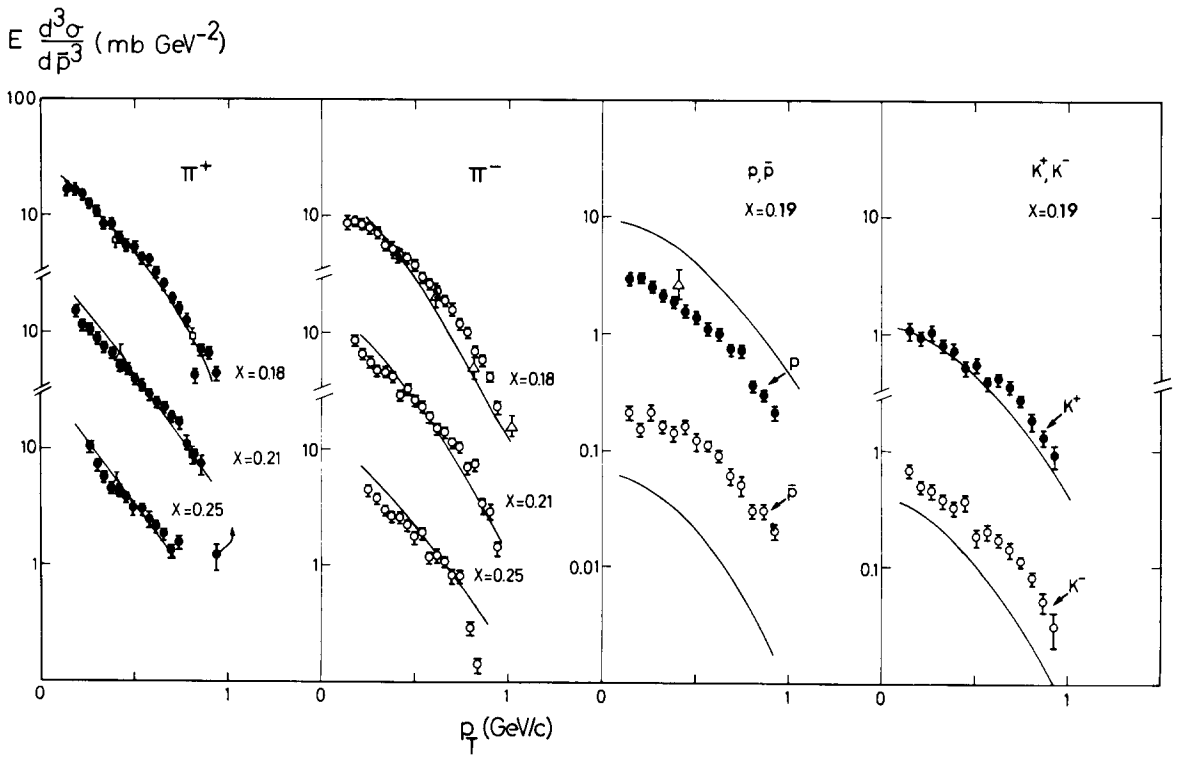

Fig. 2. Invariant cross-section for $p+p \to \pi^{\pm}+ \ldots$ at a total centre of mass energy of 53 GeV at $x = 0.18, 0.21, 0.25$ and for $p+p \to K^{\pm}+ \ldots$, $p+p \to p+ \ldots$, $p+p \to \bar{p}+ \ldots$ at $x = 0.19$; also indicated are data points from Ratner et al. [3] at 31 GeV (△) and 45 GeV (□) at $x = 0.2$ and Bertin et al. [4] at 53 GeV at $x = 0.19$ (△). The solid line represents interpolated accelerator data at 19.2 GeV/c from Allaby et al. [5]. The x value fo these latter data has been defined as $x = p/p_{max}$.

threshold was at 6.1 GeV/c. The counter C_3 (6.3 m long, 5.5 kg/cm^2 hydrogen) counted π's only in the range $3.8 < p < 12.0$ GeV/c (kaon threshold). Of the eight possible on/off combinations, three identified π's, K's and protons unambiguously in the range $3.8 < p < 6.1$ GeV/c. The remaining five combinations (0.4% of the events) arise from δ-rays produced by protons in C_1, C_2 or C_3 and/or from inefficiency of C_1 and C_2. From the appropriate combinations the efficiencies of C_1 and C_2 were measured to be greater than 99.98%. The probability of δ-ray production by protons is less than 6.10^{-4} per kg/cm^2 ethylene. The efficiency of C_3 has been measured prior to installation at the ISR to be greater than 99.5%. The possible effect of a 0.5% inefficiency on the cross-sections for kaons is less than 5%. Above 6.1 GeV/c pions are identified using C_3 only; kaons and protons are not distinguished and are rejected. The performance of C_1, C_2 and C_3 was furthermore monitored by checking that the pulse heights spectra remained stable with time.

Measurements were made of the contamination of the pion spectra by electrons by setting C_3 to 0.5 kg/cm^2 (below the muon threshold). At p_T = = 250 MeV/c the e^+/π^+ ratio was (1.1 ± 0.3)%, at p_T = 600 MeV/c the e^-/π^- ratio was (0.5 ± 0.2)%, both averaged over the p_T band accepted.

The data were further corrected for absorption in the walls of the ISR vacuum chamber (average thickness traversed 1 mm), the walls and gas of the Cerenkov counters, the scintillators and the air in the spectrometer; the correction factors were 18% for pions and negative kaons, 15% for positive kaons, 25% for protons and 35% for antiprotons for momenta between 3 and 7 GeV/c. Pions and kaons were corrected for decay in the 30 m long spectrometer; the multiplicative correction factor was 1.12 for pions and varied between 2.32 and 1.88 for kaons with

Table 1
Coefficients A, from fits to the data with the formula $E\,d^3\sigma/d\bar{p}^3 = A \exp(-Bp_T^2)$

Particle	x	A (mb/GeV^2)	B (GeV^{-2})
	0.18	16.1 ± 1.1	4.27 ± 0.16
π^+	0.21	12.9 ± 0.9	4.17 ± 0.19
	0.25	9.2 ± 0.8	3.80 ± 0.31
	0.18	9.8 ± 0.3	3.92 ± 0.07
π^-	0.21	7.6 ± 0.5	4.05 ± 0.15
	0.25	5.0 ± 0.4	3.74 ± 0.28
K^+	0.19	1.11 ± 0.05	2.75 ± 0.13
K^-	0.19	0.56 ± 0.03	3.09 ± 0.15
p	0.19	3.15 ± 0.13	3.09 ± 0.10
$\bar{p}$	0.19	0.23 ± 0.02	2.77 ± 0.19

momenta between 4.5 and 6.1 GeV/c. At each setting of the spectrometer the acceptance was determined as a function of transverse and longitudinal momentum by Monte Carlo calculations, taking into account the positions and shapes of the ISR beams appropriate for each data taking period. Only data taken in intervals of longitudinal (p_L) and transverse momenta (p_T) for which the acceptance was greater than 30% of its peak value have been used in computing the cross-sections.

The data were normalized by means of the number of coincidences in the luminosity telescope preceding each recorded event. The rate in this telescope is proportional to the luminosity, and the proportionally constant was determined periodically by the v.d. Meer method [2]. The normalization was corrected for triggers from particles going outside the apertures defined in the acceptance calculations.

The $\pi^\pm$, $K^\pm$, p and $\bar{p}$ invariant cross-sections obtained are shown in fig. 2 as a function of p_T. The errors shown are the quadratic sum of the statistical errors and a 10% systematic error arising partly from the error in the luminosity constant and partly from an uncertainty in the Monte Carlo acceptance calculation.

The following features emerge from the data:
In the measured interval of the transverse momentum p_T all distributions can be parametrized with an exponential dependence on p_T^2:

$$E\,d^3\sigma/d\bar{p}^3 = A \exp(-Bp_T^2)$$

Fitted values of A and B are given in table 1. As seen from this table the slope parameters are approximately equal for possitive and negative pions; for $K^\pm$, $\bar{p}$ and p they are significantly smaller. The average transverse momentum, which is equal to $1/(\pi B)^{1/2}$ in this parametrization, is increasing with the mass of particle. Alternative parametrizations for the p_T dependence have been suggested. It can be seen from fig. 2 that an exponential in p_T is not favoured by the present data. One obtains a qualitative description of the data with the following dependence on p_T:

$$E\,d^3\sigma/d\bar{p}^3 = C \exp(-D(m^2 + p_T^2)^{1/2}),$$

when D is kept the same for all particles. The present data can be compared with earlier ISR data from the medium angle spectrometer [3, 4]. The measurements agree within the quoted errors. The lines drawn in fig. 2 are derived from interpolation of accelerator data at 19.2 GeV/c by Allaby et al. [5]. The degree of agreement with these data is a test of scaling, i.e., energy independence of the invariant cross-section, for fixed x and p_T. One sees that scaling is particularly well satisfied by the π^+ data, perhaps somewhat less so for π^- and K^+. For K^- and $\bar{p}$ the invariant cross-section rises considerably between $s = 40$ and $s = \simeq 2810$ GeV^2 while for protons it decreases. The p_T dependence for π^- is similar to that for π^+, in contrast to the data at 19 GeV for which this dependence is different. The p_T dependence of the present data is generally flatter than at accelerator energies. For all particles the p_T dependence is also flatter than is observed near $x = 0$ [6] and $x = 0.076$ [3, 4] at ISR.

References

[1] M.G. Albrow et al., Phys. Lett. 40B (1972) 136.
[2] S. van der Meer, CERN Internal Report, ISR-PO/68-31 (1968).
[3] L.G. Ratner et al., Phys. Rev. Lett. 27 (1971) 68, and to be published.
[4] A. Bertin et al. Phys. Lett. 38B (1972) 260.
[5] J.V. Allaby, Fourth Intern. Conf. on High energy collisions, Oxford, England (1972).
[6] E. Lillethum, Fourth Intern. Conf. on High energy collisions, Oxford, England (1972).